**Preferred citation:** C.T.J. Dodson and W.W. Sampson. Effect of correlated free fibre lengths on pore size distribution in fibrous mats. In **Advances in Paper Science and Technology**, *Trans. of the XIIIth Fund. Res. Symp. Cambridge, 2005*, (S.J. I'Anson, ed.), pp 943–960, FRC, Manchester, 2018.
DOI: 10.15376/frc.2005.2.943.

# EFFECT OF CORRELATED FREE FIBRE LENGTHS ON PORE SIZE DISTRIBUTION IN FIBROUS MATS

*C.T.J. Dodson[1] and W.W. Sampson[2]*

[1] School of Mathematics,
[2]School of Materials, University of Manchester, PO Box 88,
Manchester, M60 1QD, UK.

## ABSTRACT

We provide a simulator for a range of bivariate stochastic processes of various application in the physics of stochastic fibrous networks. We illustrate the effects of local correlation on the statistics of voids in the bulk and the surface of fibre mats in general and paper in particular. The reference case of random isotropy has an inherent 'ground-state' correlation of adjacent free-fibre-lengths; this explains the classical observation of Corte that pores seem mainly 'roundish' in real paper samples. In the isotropic case, the mean pore radius can be reduced from that in a random network by 20% through structural changes associated with increased flocculation. The mean eccentricity of pores seems to give a measure of the variability in free-fibre-length distributions that is not due to local correlation. We find a uniform effect of local correlation on mean pore eccentricity over a range of stochastic network structures; at a given correlation, increased flocculation increases mean eccentricity slightly.

## INTRODUCTION

In the third of this series of symposia, Corte and Lloyd [1] presented a model for the distribution of pore radii in random fibrous networks. Miles [2] had previously shown that the expected number of sides per polygon in such a network was four and with Kallmes, Corte had shown that free-fibre-lengths, *i.e.* the lengths of the sides of polygons, had a negative exponential distribution [3]. Accordingly, Corte and Lloyd derived the probability density function for the area of rectangles given by the product of a pair of independent and identical negative exponential distributions to represent the sides of the rectangles; they proceeded to derive the probability density function for the radii of circles with the same area as these rectangles. The resulting equations showed the standard deviation of pore radii to be proportional to the mean pore radius and this was confirmed by their own experimental data and subsequently by that of Bliesner [4].

Now, whereas Corte and Lloyd's theory was derived for random fibre networks, much of the data used for verification arose from experimental measurements made on flocculated networks, *i.e.* those that were manifestly non-random. Dodson and Sampson noted that there was some evidence that the free-fibre-length in non-random fibre networks could be described by the gamma distribution and they rederived the method of Corte and Lloyd for this condition [5]. The gamma distribution has probability density

$$f(x) = \left(\frac{\alpha}{\beta}\right)^{\alpha} \frac{x^{\alpha-1}}{\Gamma(\alpha)} e^{-\alpha x/\beta} \tag{1}$$

with mean $\bar{x} = \beta$ and coefficient of variation $CV(x) = 1/\sqrt{\alpha}$; the negative exponential distribution, as used by Corte and Lloyd [1], is a special case of the gamma distribution with $\alpha = 1$.

The theory of Dodson and Sampson gives the probability density of pore radii as

$$g(r) = \left(\frac{\alpha}{\beta}\right)^{2\alpha} \frac{4\pi^{\alpha} r^{2\alpha-1} K_0(\zeta)}{\Gamma(\alpha)^2} \quad , \qquad \text{where } \zeta = 2\sqrt{\pi}\, r\, \alpha/\beta \tag{2}$$

and $K_0(\zeta)$ is the zeroth order modified Bessel function of the second kind. We note that the theory of Dodson and Sampson includes that of Corte and Lloyd as a special case when $\alpha = 1$. Also, the probability density of pore radii given by Equation (2) is itself well approximated by a gamma distribution

with the same mean and variance. Note also that in the range of application to the free-fibre-lengths and pore sizes in paper, the gamma distribution is well approximated by the lognormal distribution [1, 5] which has probability density:

$$f(r) = \frac{1}{\sqrt{2\pi}\sigma r} e^{-\frac{(\mu - \log(x))^2}{2\sigma^2}} \tag{3}$$

with mean $\bar{r} = e^{\mu+\sigma^2/2}$ and coefficient of variation $CV(r) = \sqrt{e^{\sigma^2} - 1}$. For $r$ with lognormal probability density given by Equation (3), $\log(r)$ exhibits a Gaussian distribution with mean $\overline{\log(r)} = \mu$ and coefficient of variation $CV(\log(r)) = \sigma/\mu$.

Note that the property of having sample coefficient of variation independent of the mean actually characterizes gamma distributions, as shown recently by Hwang and Hu [6]. Whereas there is a growing body of evidence confirming the suitability of the gamma distribution to describe the dimensions of voids in paper [7, 9, 10], and in general classes of stochastic porous material [11, 12], the influence on physical phenomena of the parameters characterising the distribution has yet to be satisfactorily explained. In part this arises because, whereas the derivations for the probability density functions for pore areas and hence for pore radii assume that adjacent polygon sides have independent lengths, in practice they do not. This observation was made by Corte and Lloyd [1] who noted that 'roundish' hence more regular polygons are more frequent than oblong ones, and that 'slit-shaped' polygons are extremely rare [13]. There are analytic results of Miles [2]: the expected fraction of polygons that are triangles is $(2 - \pi^2/6) \approx 0.355$, and the perimeter of polygons with $n$ sides has a $\chi^2$ distribution with $2(n - 2)$ degrees of freedom. Interestingly, $\chi^2$ distributions with 2,3, . . . degrees of freedom closely resemble gamma distributions; indeed, the $n = 3$ case for triangles coincides precisely with an exponential distribution, cf. [8] Figure 2.11. Note that for independent free fibre lengths following a *Gaussian* distribution the perimeter distributions for $n$-sided polygons would be $\chi^2$ with $n - 1$ degrees of freedom—so for triangles it gives the same as Miles [2], but the Gaussian case differs somewhat for larger $n$. Simulations of Piekaar and Clarenburg [14] found that around 39 % of the polygons are triangles, around 35 % have four sides and the remaining 25 % or so have 5 or more sides in the random isotropic case.

## CORRELATION

Graphical representations of two stochastic fibre networks are given in Figure 1; the histogram beneath each network shows the distribution of orientations of fibres in that network. Each network consists of 1500 fibres of length 1 *mm* with their centres randomly positioned within a square of side 1 *cm* and in the image on the left, the fibre orientation distribution is uniform. In the image on the right, the locations of the fibre centres are the same and fibre axes are preferentially oriented towards the vertical.

Consider first the isotropic network on the left of Figure 1. First inspection reveals that in regions of high density there are many short free-fibre-lengths, and that in regions of low density there are fewer but longer free-fibre-lengths. So we have positive correlation between nearby polygonal side

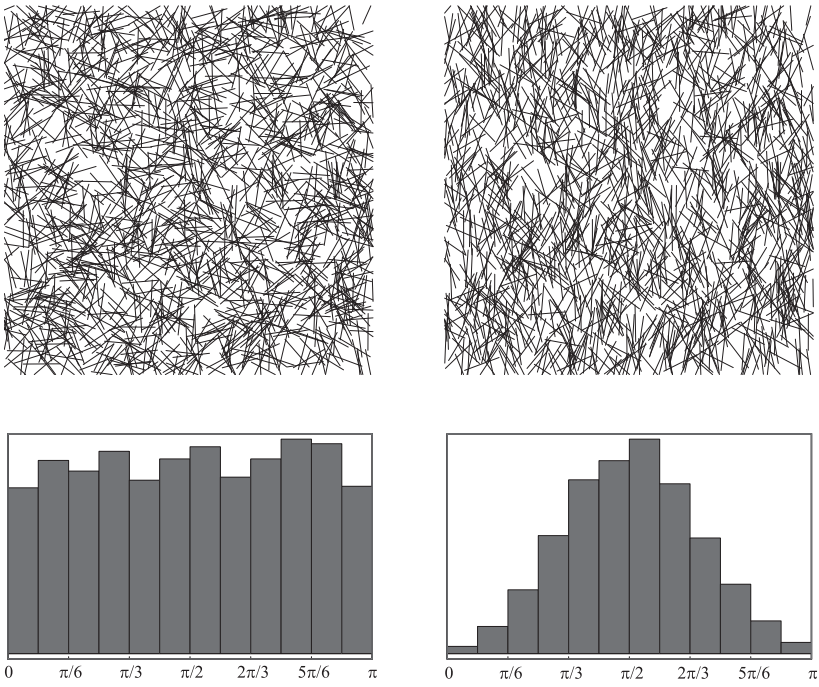


**Figure 1** Networks of 1500 fibres of length 1 *mm* with centres randomly positioned within a square of side 1 *cm*. On the left, fibre axes have a uniform orientation; on the right, fibre axes are preferentially oriented towards the vertical direction. The locations of fibre centres in each image are the same.

lengths and this tends to yield more regular polygons, simply from the random variations in the local density that arise from the underlying Poisson point process for fibre centres. Random isotropy has an inherent 'ground-state' correlation of adjacent free-fibre-lengths, why pores seem mainly 'roundish' in real paper samples. Consider now the oriented network on the right; in this case we still see the effects of the local density of crossings on the lengths of nearby sides, but we observe fewer 'roundish' polygons and more polygons of appreciable aspect ratio. It is important to note however that even in the oriented example shown here, the correlation between pairs of adjacent polygon sides remains positive; so the effect of random variations in the local density overwhelms the superposed anisotropy. For a significant fraction of polygons to be 'slit-shaped', we require pairs of adjacent polygon sides to consist of one short side and one long side. In this case, we require strong negative correlation and this is unlikely in stochastic fibre networks since the clustering of fibre centres inherent in such structures favours positive correlation.

Here we study the influence of the degree of correlation between the lengths of adjacent free-fibre-lengths on the statistics describing the distribution of pore sizes in the thin fibre networks. We have developed computer routines that generate pairs of random numbers distributed according to two families of bivariate distributions that each permit different degrees of correlation, $\rho$. Firstly, we consider pairs of polygon sides distributed according to a bivariate lognormal distribution with $-1 \leq \rho \leq 1$. Next we generated pairs of polygon sides distributed according to the McKay bivariate gamma distribution which allows positive correlation $0 < \rho \leq 1$; we do not have analytically a bivariate gamma distribution with negative correlation. However, we provide some analytic results from several other analytic statistical models that yield several distributions of correlated free-fibre lengths.

## THEORY

Existing theory [5] gives the probability density function for the area $a$ of rectangles with independent, *i.e.* uncorrelated, and identically gamma distributed sides $x$ and $y$ such that $a = xy$. We consider two cases, first pairs of correlated $x$ and $y$ where the distributions of $x$ and $y$ are identical; we consider this case to represent isotropic correlated networks. The second case we consider is one where the distributions of $x$ and $y$ are determined by the correlation coefficient, then the mean and variance of the two distributions are not equal; we consider these to represent oriented networks where the orientation and correlation are coupled.

**Case 1: Isotropic correlated networks**

Consider first a special case where the distribution of free-fibre-lengths is lognormal and has unit mean $\bar{x} = \bar{y} = 1$; this makes the total free-fibre-length constant: $\bar{x} + \bar{y} = 2$. Also, we constrain the problem such that the coefficients of variation of $x$ and $y$ are equal, *i.e.* $CV(x) = CV(y)$. To generate pairs of lognormally distributed numbers, we generate first pairs of numbers, $(X, Y)$ with a bivariate Gaussian distribution and these represent $(\log(x), \log(y))$. Since $\bar{x} = \bar{y} = 1$, we have from Equation (3),

$$\sigma(X) = \sigma(Y) \quad = \quad \sqrt{\log\left(1 + CV(x)^2\right)} \tag{4}$$

$$\overline{\log(x)} = \overline{\log(y)} = \bar{X} = \bar{Y} \quad = \quad -\frac{\sigma(X)^2}{2} \quad , \tag{5}$$

and the joint probability density of $X$ and $Y$ with correlation coefficient $\rho$ is the bivariate Gaussian,

$$g(X,Y;\sigma(X),\rho) = \frac{e^{\frac{2(X^2+Y^2-2XY\rho)+2(X+Y)(1-\rho)\sigma(X)^2+(1-\rho)\sigma(X)^4}{4(\rho^2-1)\sigma(X)^2}}}{2\pi\sqrt{(1-\rho^2)\sigma(X)}} \tag{6}$$

In Equation (6), parameter $\rho$ quantifies the correlation between Gaussian $X$ and $Y$; this controls the correlation between lognormal $x$ and $y$ so in simulations the desired correlation for the lognormal variables is achieved by successive adjustments to the input bivariate Gaussian.

The computer algebra software, *Mathematica* [15] includes optimised code to generate pairs of random numbers with a bivariate Gaussian distribution. We used this code to generate 5000 pairs of numbers for a range of $\rho$ and $CV(x)$ and from these generated pairs of lognormally distributed $x$ and $y$. Example families of bivariate lognormal pairs of numbers $(x,y)$ with strong and weak positive and negative correlation are shown in Figure 2 for the case with $CV(x) = CV(y) = 1$.

*Pore statistics*

Pores are modelled as ellipses, each characterised by a pair of $x$ and $y$ that represent its minor and major axes respectively. The eccentricity of each pore is given by,

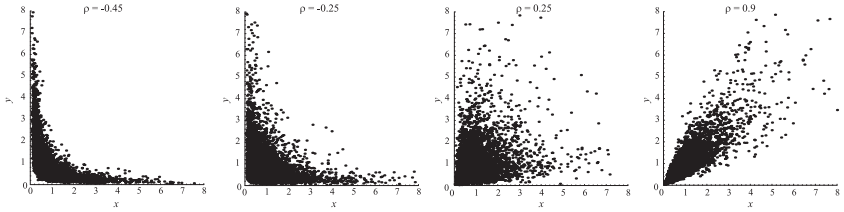


**Figure 2** Four outputs of the bivariate lognormal generator with differing degrees of positive and negative correlation. Each family of pairs of $x$ and $y$ has $CV(x) = CV(y) = 1$.

$$\varepsilon = \sqrt{1 - \left(\frac{x}{y}\right)^2} \tag{7}$$

and as a rule of thumb, we can consider pores to be 'roundish' if they have eccentricity less than about 0.6. The area of an elliptical pore is given by

$$A = \pi x y \ , \tag{8}$$

and its perimeter is,

$$P = 4\,y\,E(\varepsilon^2) \tag{9}$$

where $E(\varepsilon^2)$ is the complete elliptic integral.

The parameter of primary interest to us here is the equivalent radius of each pore and this is given by,

$$r = 2\frac{A}{P} \ . \tag{10}$$

Thus, using each generated pair of correlated $x$ and $y$ we calculate the eccentricity, area, perimeter and hence the equivalent radius of a pore. Then we calculate the statistics describing the distribution of these parameters for 5000 pores over a range of values of $\rho$ and $CV(x)$.

The influence of correlation on pore shape, as characterised by the mean eccentricity, $\bar{\varepsilon}$ is shown in Figure 3. The figure includes diagrams of ellipses with a range of eccentricities to aid interpretation of the data. As anticipated, the propensity of voids in the network to be 'roundish', $\bar{\varepsilon} < 0.6$, increases as correlation gets close to unity. Note that the correlation coefficient $\rho$ plotted in Figure 3 is that calculated for the lognormally distributed data $(x,y)$.

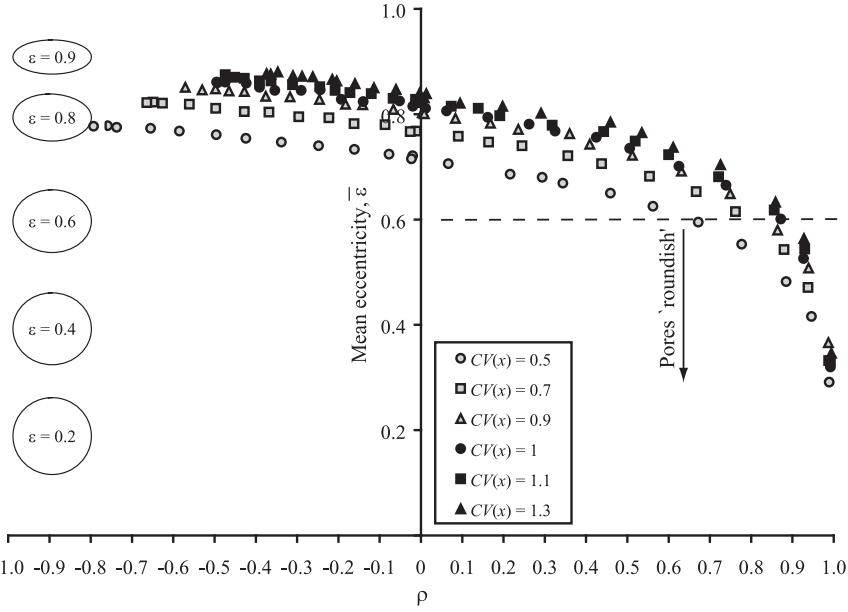


**Figure 3** Influence of correlation on the pore eccentricity using the bivariate lognormal distribution for free-fibre-lengths. The graphical key on the left of the figure shows ellipses with eccentricity between 0.2 and 0.9. 'Roundish' pores are those with eccentricity less than 0.6.

We expect the coefficient of variation of free-fibre-lengths $CV(x)$ to measure to some extent the uniformity of the network, $CV(x) = 1$ approximating to the random case. Thus a network with $CV(x) > 1$ is expected to correspond to a more flocculated network and $CV(x) < 1$ corresponds to greater uniformity than random. Figure 3 shows that at a given correlation, the mean eccentricity of pores increases with increasing $CV(x)$. Intuitively, positive correlation of adjacent free-fibre-lengths would be increased by flocculation and negative correlation would be increased by anisotropy. It follows that if 'roundish' pores are observed then there is little local variability in $y$ that is not due to variability in $x$; in other words, variations in local density control the local correlation and force roundish pores to predominate.

The standard deviation of eccentricity is plotted against the mean eccentricity in Figure 4. We observe that as the mean eccentricity decreases with increasing correlation, then the standard deviation of eccentricity decreases also. This agrees with the observation of Corte and Lloyd that not only are

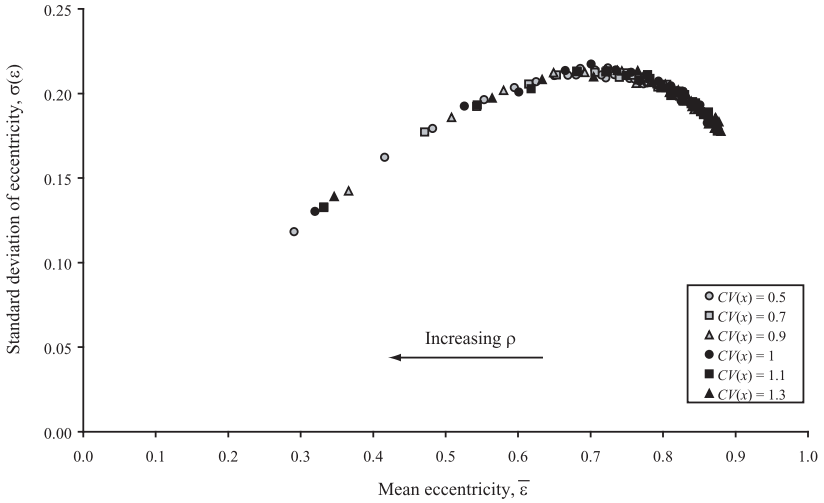


**Figure 4** Standard deviation of eccentricity plotted against mean eccentricity using bivariate lognormal distribution of free-fibre-lengths.

pores roundish, but that few are slit-shaped. It is interesting to note also that there is no significant effect of the coefficient of variation of free-fibre-length on the relationship between the standard deviation and mean eccentricities and that the data exhibit a maximum when $\bar{\varepsilon}$ is about 0.7.

The mean pore radius is plotted against the correlation coefficient $\rho$ in Figure 5. Recall that as correlation increases so does the propensity of pores to be roundish. Thus, in Figure 5 we see that the mean radius of pores increases as pores tend to be more roundish with increasing correlation. Note that in the high positively correlated cases, there is little influence of the coefficient of variation of free-fibre-length, suggesting that the influence of formation on the mean pore size is weak; such weak dependencies are consistent with data reported in the literature [9]. Recall that the uncorrelated case, the datapoints lying on the axis $\rho = 0$, represents that considered by existing models [5] and these show much greater sensitivity to the $CV(x)$.

### Case 2: Dependent correlation and anisotropy

For correlated $x$ and $y$ with $\bar{x} \neq \bar{y}$ we use the McKay bivariate gamma distribution with joint probability density,

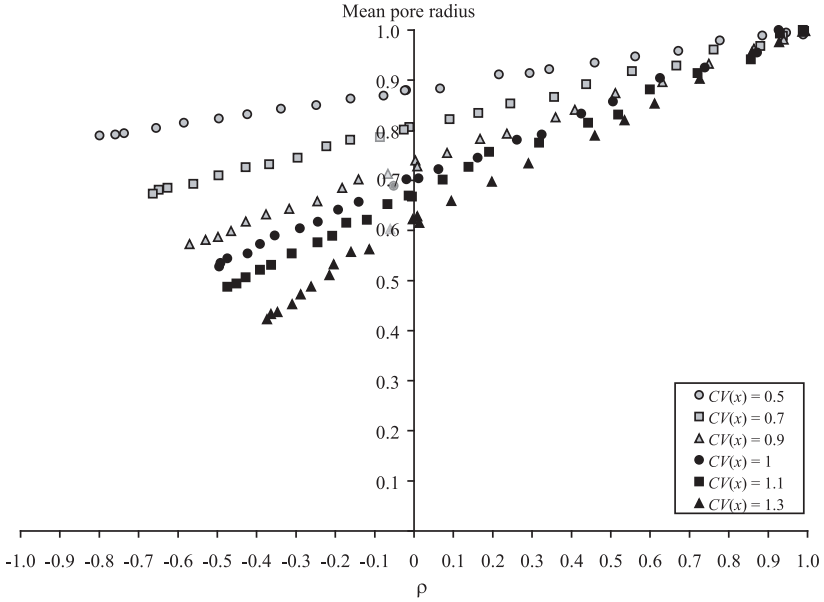


**Figure 5** Influence of correlation on the mean pore radius for lognormal distributions of free-fibre-lengths.

$$m(x,y;a_1,\sigma_{12},a_2) = \frac{(\frac{a_1}{\sigma_{12}})^{\frac{(a_1+a_2)}{2}} x^{a_1-1}(y-x)^{a_2-1} e^{-\sqrt{\frac{a_1}{\sigma_{12}}}y}}{\Gamma(a_1)\Gamma(a_2)} \quad , \tag{11}$$

where $0 < x < y < \infty$ and $a_1$, $\sigma_{12}$, $a_2 > 0$. Whereas the distribution requires $y > x$, we may use it to model correlated polygon sides since the ordering of polygon sides is arbitrary.

The marginal probability densities of $x$ and $y$ are univariate gamma distributions with,

$$\bar{x} = \sqrt{a_1 \sigma_{12}} \tag{12}$$

$$\bar{y} = (a_1 + a_2)\sqrt{\frac{\sigma_{12}}{a_1}} \quad . \tag{13}$$

The correlation coefficient between $x$ and $y$ is given by,

$$\rho = \sqrt{\frac{a_1}{a_1 + a_2}} \quad . \tag{14}$$

As before, we need to keep the total free-fibre-length constant, so we want $\bar{x} + \bar{y} = 2$. From Equation (12) we have,

$$\bar{y} = 2 - \sqrt{a_1\, \sigma_{12}} \quad . \tag{15}$$

Equating Equations (15) and (13) yields, on manipulation,

$$a_2 = 2\left(\sqrt{\frac{a_1}{\sigma_{12}}} - a_1\right) \quad , \tag{16}$$

and from Equation (12) we have,

$$a_1 = \frac{\bar{x}^2}{\sigma_{12}} \quad . \tag{17}$$

On simplification, substitution of Equations (16) and (17) in Equation (14) yields

$$\begin{aligned} \rho &= \sqrt{\frac{\bar{x}}{2 - \bar{x}}} \\ &= \sqrt{\frac{\bar{x}}{\bar{y}}} \quad . \end{aligned} \tag{18}$$

It follows directly that

$$\bar{x} = \frac{2\rho^2}{1 + \rho^2} \qquad \text{and} \qquad \bar{y} = \frac{2}{1 + \rho^2} \tag{19}$$

such that

$$\bar{x} + \bar{y} = 2 \quad .$$

The variances of $x$ and $y$ are given by,

$$\sigma^2(x) = \frac{\bar{x}}{a_1} \tag{20}$$

$$\sigma^2(y) = \frac{\bar{y}}{a_1 + a_2} \ , \tag{21}$$

respectively, and from Equation (14) we have

$$a_2 = a_1 \left( \frac{1}{\rho^2} - 1 \right) \ . \tag{22}$$

Substitution of Equations (19) and (22) in Equations (20) and (21) respectively yields,

$$\sigma^2(x) = \frac{4\rho^4}{(1+\rho^2)^2\, a_1} \tag{23}$$

$$\sigma^2(y) = \frac{4\rho^2}{(1+\rho^2)^2\, a_1} \ , \tag{24}$$

such that

$$\sigma^2(x) = \rho^2\, \sigma^2(y) \ .$$

By specifying the correlation coefficient $\rho$ and the coefficient of variation of $x$ ($CV(x) = \frac{\sigma_x}{\bar{x}} = \frac{1}{\sqrt{a_1}}$) we fully define the marginal and joint pdf's of $x$ and $y$:

$$\begin{aligned} a_1 &= \frac{1}{CV(x)^2} \\ a_2 &= a_1 \left( \frac{1}{\rho^2} - 1 \right) \\ \bar{x} &= \frac{2\rho^2}{1+\rho^2} \\ \bar{y} &= \frac{2}{1+\rho^2} \\ \sigma_{12} &= \frac{\bar{x}^2}{a_1} \end{aligned}$$

It is easy to show that

$$CV(y) = \rho\, CV(x) \;\text{ hence } CV(y) < CV(x) = \frac{1}{\sqrt{a_1}} \;.$$

We have written code to generate pairs of $x$ and $y$ distributed according to the McKay bivariate gamma distribution as given by Equation (11) and we use the generated pairs to compute the structural characteristics of voids as discussed previously for the isotropic case. The inputs to the routine are the target values of the correlation coefficient, $\rho$ and the coefficient of variation of $x$.

To generate the McKay distributed pairs, we compute first the fraction of all $x$-$y$ pairs in a given square region of the $x$-$y$ plane; this is given by,

$$P(x,y) = \int_{x}^{x+\Delta x} \int_{y}^{y+\Delta y} m(x,y)\, dy\, dx \tag{25}$$

This integral is evaluated numerically for a range of $x$ and $y$ sufficient to characterise the full distribution. These fractions multiplied by the required number of pairs of $x$ and $y$ define the number of points in each region; and the routine generates this number of pairs of uniformly distributed random numbers in the interval $(x + \Delta x, y + \Delta y)$ for each square region of interest. In the simulations presented here, intervals of $\Delta x = \Delta y = 0.1$ have been sufficient to yield McKay distributed pairs of $x$ and $y$ with $\rho$ within 3 % of the input. Examples of the outputs of the generator are shown in Figure 6 where each plot shows 5000 points each representing an $x$-$y$ pair.

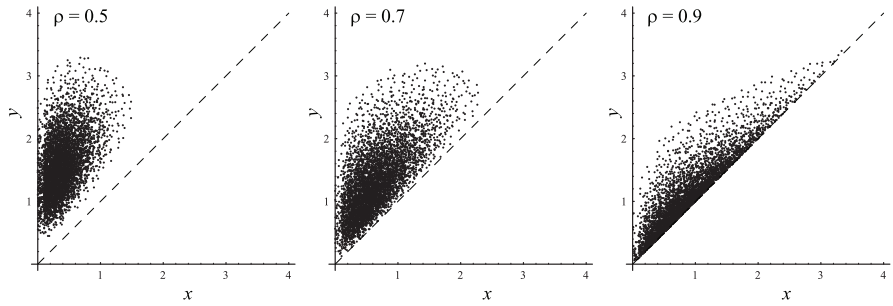


**Figure 6** Three outputs of the McKay generator with differing degrees of correlation. Each family of pairs of $x$ and $y$ has $CV(x) = 0.6$.

*Pore statistics*

The simulator has been used to compute the statistics of elliptical voids for a range of correlation coefficients and a range of $CV(x)$. Each time the simulator was run, 5000 pairs of $x$ and $y$ and the coefficient of variation of all $x$ and $y$, $CV(x \cup y)$ were computed from the resulting data.

The mean eccentricity is plotted against the correlation coefficient in Figure 7. In this, and all figures arising from our analysis of the McKay bivariate gamma distribution, we present data where $\bar{\varepsilon} \leq 0.95$; these being associated with correlation coefficients greater than about 0.5. Note that in the isotropic correlated case, the greatest value of $\bar{\varepsilon}$ observed was around 0.8. We observe a similar relationship to the lognormal case with positive correlation, cf. Figure 3. However, here we have a curve rather like

$$\bar{\varepsilon}^2 = 1 - \rho^2$$

so $\bar{\varepsilon}$ essentially measures the variation in $y$ not due to positive linear correlation with $x$.

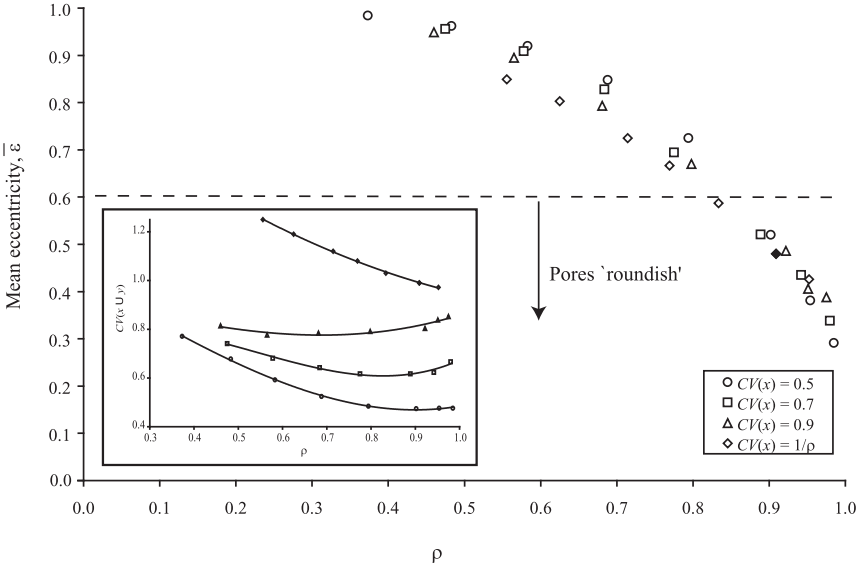


**Figure 7** Influence of correlation on pore eccentricity using the McKay bivariate gamma distribution for free-fibre-lengths. Inset figure shows $CV(x \cup y)$ plotted against correlation. The filled point has $CV(x \cup y) = 0.99$ and thus represents a case close to a random network.

The sensitivity to $CV(x)$ is less than in the lognormal case and this arises partly because the coefficients of variation of $x$ and $y$ are no longer equal. Network uniformity is better characterised by $CV(x \cup y)$, though this is a function of $\rho$ and $CV(x)$ also as illustrated in the inset plot. Importantly, the ranking of $CV(x \cup y)$ is the same as that of $CV(x)$ so this may still be used as an approximate measure of uniformity.

The standard deviation of eccentricities is plotted against the mean eccentricity in Figure 8. Here we observe a stronger maximum than that seen in Figure 4 for the bivariate lognormal distribution and a much stronger dependence on the uniformity of the network as characterised by $CV(x)$.

Note that when the average eccentricity is less than 0.6, and hence pores may be considered typically 'roundish', the standard deviation of eccentricities is greater than in the isotropic case, *i.e.* there is a greater likelihood of finding slit-shaped pores when the standard deviation of eccentricities is greater.

The mean pore radius is plotted against the correlation coefficient in Figure 9 and, as was observed in Figure 5, the mean pore radius increases with increasing correlation and propensity for pores to be round. The effect

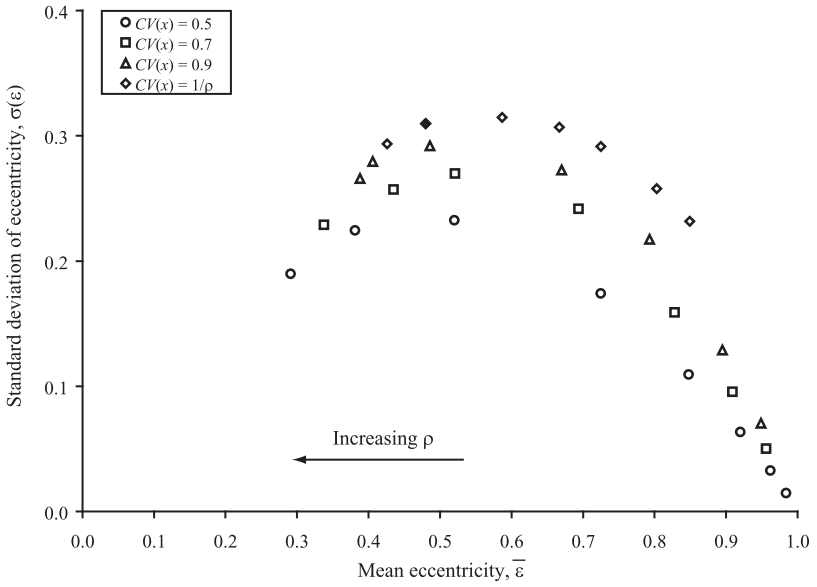


**Figure 8** Standard Deviation of eccentricity plotted against mean eccentricity using the McKay bivariate gamma distribution for free-fibre-lengths. The filled point has $CV(x \cup y) = 0.99$ and thus represents a case close to a random network.

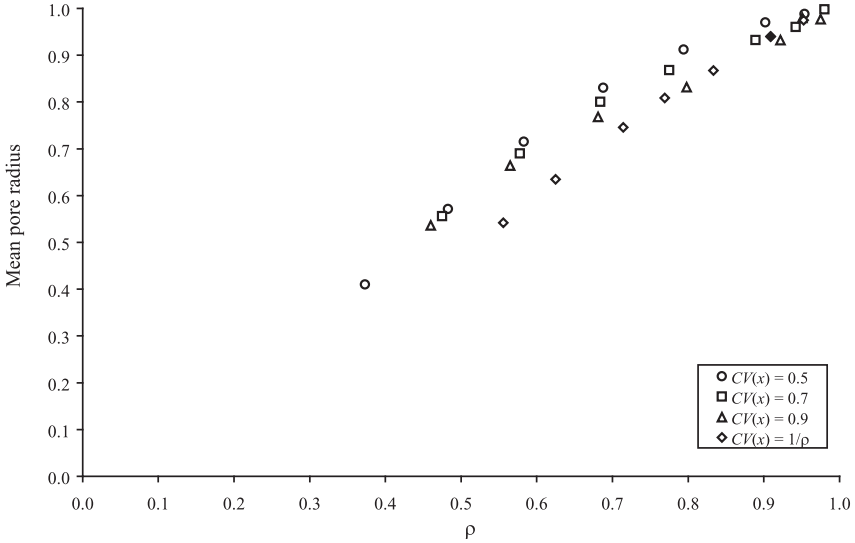


**Figure 9** Influence of correlation on the mean pore radius using McKay bivariate gamma distribution for free-fibre-lengths. The filled point has $CV(x \cup y) = 0.99$ and thus represents a case close to a random network.

here is stronger than that observed in the isotropic case since the dependence of the mean eccentricity on correlation is greater.

## SIMPLE ANALYTIC MODELS: STRONG CORRELATION

To run a check on the simulations and to see the effect of strong negative correlation on eccentricity statistics, we devised a family of simple analytic models in which pairs $(x,y)$ with $x < y$ and $x + y = 1$ arise by stochastic partitioning of the unit interval [0, 1]. The partitioning cut of the interval was made with each of three different analytic probability distributions for the positioning of the cut: two symmetric PDFs: uniform, sine, and a triangular skew PDF. The resulting distributions of eccentricities were derived analytically and all look rather like some of those obtained for lognormal and McKay simulations. Similarly simple analytic models for strong positive correlation gave similar results. Table 1 shows a summary of the analytic values for eccentricity statistics and we are encouraged to see that these results lie also on the curves from simulations using correlated lognormal (Figure 3)

**Table 1** Summary of eccentricity statistics from three different analytic models of strongly negatively and strongly positively correlated adjacent free-fibre-lengths.

| | $\rho \approx -1$ | | $\rho \approx +1$ | |
|---|---|---|---|---|
| PDF | $\bar{\varepsilon}$ | $\sigma(3)$ | $\bar{\varepsilon}$ | $\sigma(3)$ |
| Uniform | 0.858 | 0.189 | 0.941 | 0.042 |
| Sine curve | 0.793 | 0.207 | 0.942 | 0.045 |
| Skew triangle | 0.858 | 0.189 | 0.965 | 0.033 |

and correlated gamma (Figure 7). This suggests a uniform effect of local correlation on mean eccentricity over a range of stochastic network structures; at a given correlation, increased flocculation ($CV(x)$) increases mean eccentricity slightly.

## CONCLUSIONS

Previous studies of the pore size distribution in planar random fibrous networks have assumed the lengths of the adjacent sides of polygons in the network, *i.e.* adjacent free-fibre-lengths, to be independent. We have shown that a consequence of the variations of local density due to the underlying Poisson point process of fibre centres, is that polygon sides are correlated; this effect is sufficiently strong that it may overwhelm any effect of the orientation of fibre axes and forces the correlation to be positive.

We have used numerical techniques to generate statistics characterising the pore size and shape in networks with correlated free-fibre-lengths distributed according to the bivariate lognormal and the McKay bivariate gamma distributions. Our simulations show that the reference case of random isotropy has an inherent 'ground-state' correlation of adjacent free-fibre-lengths; this explains why pores seem mainly 'roundish' in real paper samples. In isotropic networks, the mean pore radius can be reduced from that in a random network by 20% through structural changes associated with increased flocculation; this effect is reduced with increasing positive correlation between nearby free-fibre-lengths. The mean eccentricity of pores seems to give a measure of the variability in free-fibre-length distributions that is not due to local correlation. We find a uniform effect of local correlation on mean eccentricity over a range of stochastic network structures; at a given correlation, increased flocculation increases mean eccentricity slightly.

An important practical application would be to quantify the range of

porosity structures achievable by a given manufacturing process and so specify the optimal effective ranges for control variables.

Future work will probe further the interactions of anisotropy and flocculation on correlations between adjacent free-fibre-lengths, by means of models and measurements in real networks.

## REFERENCES


1. H. Corte and E.H. Lloyd. Fluid flow through paper and sheet structure. In **Consolidation of the Paper Web** *Trans. IIIrd Fund. Res. Symp.* (F. Bolam, ed.), pp981–1009, BPBMA, London, 1966.
2. R.E. Miles. Random polygons determined by random lines in a plane. *Proc. Nat. Acad. Sci. USA* **52**:901–907,1157–1160, 1964.
3. H. Corte and O.J. Kallmes. Statistical geometry of a fibrous network. In **The Formation and Structure of Paper**, *Trans. IInd Fund. Res. Symp.*, (F. Bolam, ed.), pp13–46, Tech. Sect. BPBMA, London 1962.
4. W.C. Bliesner. A study of the porous structure of fibrous sheets using permeability techniques. *Tappi J.* **47** (7):392–400, 1964.
5. C.T.J. Dodson and W.W. Sampson. The effect of paper formation and grammage on its pore size distribution. *J. Pulp Pap. Sci.* **22**(5):J165–J169, 1996.
6. T-Y. Hwang and C-Y. Hu. On a characterization of the gamma distribution: The independence of the sample mean and the sample coefficient of variation. *Annals Inst. Statist. Math.* 51, 4 (1999) 749–753.
7. J. Castro and M. Ostoja-Starzewski. Particle sieving in a random fiber network. *Appl. Math. Modelling* **24**(8–9):523–534, 2000.
8. M. Deng and C.T.J. Dodson. **Paper: An Engineered Stochastic Structure**. Tappi Press, Atlanta 1994.
9. C.T.J. Dodson, A.G. Handley, Y. Oba and W.W. Sampson. The pore radius distribution in paper. Part I: The effect of formation and grammage. *Appita J.* **56**(4):275–280, 2003.
10. W.W. Sampson. Comments on the pore radius distribution in near-planar stochastic fibre networks. *J. Mater. Sci.* **36**(21):5131–5135, 2001.
11. P.R. Johnston. The most probable pore size distribution in fluid filter media. *J. Test. and Eval.* **11**(2):117–121, 1983.
12. P.R. Johnston. Revisiting the most probable pore size distribution in filter media. The gamma distribution. *Filtrn. and Sepn.* **35**(3):287–292, 1998.
13. H. Corte. Statistical geometry of random fibre networks. In **Structure, Solid Mechanics and Engineering Design**, Proc. Southampton 1969 Civil Engineering Materials Conference, vol. 1, (ed. M. Te'eni):pp341–355. Wiley-Interscience, London, 1971.
14. H.W. Piekaar and L.A. Clarenburg. Aerosol filters – Pore size distribution in fibrous filters. *Chem. Eng. Sci.* **22**:1399–1408, 1967.
15. S. Wolfram. **The Mathematica Book.**, 5th edition, Wolfram Media, Champaign, 2003.

# EFFECT OF CORRELATED FREE FIBRE LENGTHS ON PORE SIZE DISTRIBUTION IN FIBROUS MATS

*C.T.J. Dodson*[1] *and W.W. Sampson*[2]

[1]School of Mathematics,
[2]School of Materials, University of Manchester, PO Box 88,
Manchester, M60 1QD, UK

**Corrected Error in the Paper**

Table 1 in this paper was reproduced erroneously. The correct version is as follows:

**Table 1** Summary of eccentricity statistics from three different analytic models of strongly negative and strongly positively correlated adjacent free-fibre-lengths.

| | $\rho \approx -1$ | | $\rho \approx +1$ | |
|---|---|---|---|---|
| PDF | $\bar{\varepsilon}$ | $\sigma(\varepsilon)$ | $\bar{\varepsilon}$ | $\sigma(\varepsilon)$ |
| Uniform | 0.858 | 0.189 | 0.941 | 0.042 |
| Sine curve | 0.793 | 0.207 | 0.942 | 0.045 |
| Skew triangle | 0.858 | 0.189 | 0.965 | 0.033 |

## DISCUSSION CONTRIBUTIONS

*Patrice Mangin* U.Q.T.R./CIPP

You are hooking up your layout of fibres on the Poisson distribution basically on a flat plane. Is this also valid if you have a circle pattern? Could I

convolute your approach with a wire underneath so that I would have a slightly different distribution than the Poisson distribution or would I still have a Poisson distribution?

*Christopher Dodson*

No, in the case of gamma distributed free-fibre length, it will not have an underlying Poisson distribution except in the special case when the gamma reduces to an exponential. The gamma contains the exponential as a special case and, only when you have that special case, is it subordinate to an underlying Poisson space distribution. In the other cases it is not a Poisson space. Unfortunately, none of the other distributions, unlike the Poisson and exponential, have these complements. There is no natural space structure which corresponds to a gamma. That is the fundamental problem. It is well known.

*Richard Hoyland* University of Manchester

Are all your theoretical fibres of the same length?

*Christopher Dodson*

No, that is not necessary, although it was so in the picture. The fibres are of arbitrary length.

*Torbjørn Helle* Norwegian University of Science and Technology

You mentioned the problem of getting uniform pore dimensions in paper which Dr. Corte proved was theoretically impossible. I think I remember some work of Dr. Radvan of Wiggins Teape. He worked on a process involving mixing foam into the paper furnish before forming. The foam reduced the fibres' tendency to flocculate and the bubbles in the foam were assumed to define pore sizes. It was a fascinating idea, but I have heard that there were severe practical problems, with a mess of foam in the wet end! Do you know if there ever was a positive outcome of Dr. Radvan's work with the foam process?

*Christopher Dodson*

It was a very wet process in the lab! Yes, it did produce a different pore size distribution from normally stochastically freely formed papers, but not

extremely much so. Because it was produced at the time that I was working with Corte who was really concerned with the pore size distribution, anything that did not confirm that would have been highly publicised. There were effects and there are some data, including, I believe, some in the literature. There may also be some old reports which may be available through Peter Herdman, since I do not think they are still classified. Certainly the foam did give a different structure.

*Tetsu Uesaka* Mid Sweden University

The second statement of your concluding slide that "Mean pore radius in random networks may be reduced by 20% with increased flocculation" is very interesting. We have done a few computational simulations of fibre networks, and we do not have a direct result, but they seem to be suggesting that this effect is happening. It means pore areas seem to be reduced by increasing flocculation.

*Christopher Dodson*

So, you have actually observed that?

*Tetsu Uesaka*

I would not say it is a "direct" result. My question is: how about the frequency of the very large pores as you flocculate the system, the frequency of the occurrences of the very, very large pores? Does this decrease or increase? How does it behave?

*Christopher Dodson*

Well, that is an interesting mathematical statistics problem because the statistics of the extreme values in pore size distribution will be sensitive to the underlying bivariate distributions that represent the polygonal size. In the original case with exponential polygon size, the work was done on extreme value statistics and that was a major part of the activity in Heinz Corte's group because we wanted the first bubble to come through in the fluid permeation. So, that was important there. We have not done the statistics for the bivariate McKay. The extreme value statistics there would prove a little bit more demanding. However, I would be delighted if, in your new faculty position, you could find a student to get to grips with that. That will be a lovely project: to look at the extreme value statistics of the anisotropic, flocculated model for the networks through the pore size distribution and shape.